ACS APPLIED POLYMER MATERIALS

pubs.acs.org/acsapm Article

Photoreactivity and Enhanced Mechanical Properties and Water Stability in Polysaccharide-Based Films Using Vanadium Ion Coordination

Carina Haddad, E. A. Kalani D. Edirisinghe, Hope M. Brown, and Alexis D. Ostrowski*

Cite This: ACS Appl. Polym. Mater. 2022, 4, 859–867 Read Online

ACCESS | Metrics & More | Article Recommendations | Supporting Information

ABSTRACT: Different strategies have been employed to improve the physicochemical and mechanical properties of soft polysaccharide-based materials. Some of these strategies include covalent cross-linking or chemical modification and blending of polymers. In an alternative approach, we used vanadium ion coordination to create dynamic covalent bonds and obtain films with enhanced properties. We prepared bio-based films using pectin and chitosan, two naturally occurring polysaccharides, with glycerol added as a plasticizer to increase the flexibility and elasticity of the material. We incorporated the vanadium ion into the films via soaking in V(V) solutions. Films were characterized through FT-IR to examine the different interactions inside the films. Scanning electron microscopy showed laminated sheets separated by ∼0.16 μm in the V(V)-containing films as compared to ∼0.75 μm in the films without V(V). Rheological studies showed that V(V)-coordinated films possessed better mechanical properties (higher storage modulus) and water stability than films without vanadium. Upon irradiation with blue light, diffuse reflectance spectroscopy and color analysis showed the changes in the color of the film with irradiation from yellow to blue, consistent with the photochemical reduction of V(V) to V(IV). A small change in modulus was observed during light irradiation without significant structural changes observed within the film in scanning electron microscopy. These results show that it is possible to create robust and water-stable polysaccharide-based materials through coordination of the functional groups of polysaccharides with metal ions.

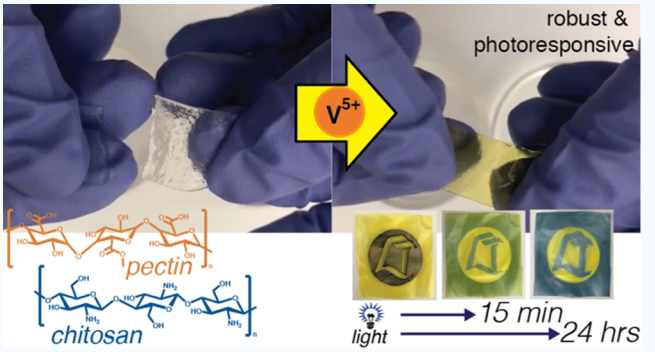

KEYWORDS: *polysaccharide, chitosan, pectin, films, vanadium, metal coordination, photochemistry*

INTRODUCTION

In recent years, bio-based composite materials have been developed to substitute petroleum-based plastics due to the lasting harmful impact of the petroleum-based plastics on the environment.[1,2] Lipids, proteins, and polysaccharides have been used to create these bio-friendly materials as a promising solution for a cleaner future.[3−7] However, studies have been more focused on the use of polysaccharides due to their diverse advantages such as low cost, high film-forming ability, low-toxicity, and abundant bioavailability.[8] The two main disadvantages of polysaccharide-based materials are first, their hydrophilic nature which makes them disintegrate quickly in water and second, their mechanically weak nature which restricts their use in different applications. To overcome these major drawbacks, blends of different polysaccharides were used to form films with enhanced physicochemical and mechanical properties. It has been shown that blend films possess better properties than films made from a single polysaccharide.[9−13] Moreover, researchers proposed adding other components to polysaccharide-based materials to create films featuring stiffness and elasticity. Citric acid, gallic acid, ferulic acid, and boric acid, for example, were added as cross-linkers to change the properties of polysaccharide films.[14−16] Nanotechnology also emerged as an approach to boost the performance of bio-based materials. Nanoparticles and nanofibers were used as nonreinforcements for that matter.[17,18] Other components such as sorbitol, glycerol, and triethyl citrate were added as plasticizers to impart stretchability.[19−21] Starch, pectin (PE), cellulose, and chitosan (CH) are among the different polysaccharides found in nature which have been extensively used to create films that contributed to different applications such as food packages, carriers for active compounds and drug delivery systems, flexible electronics, and so forth.[22−27] However, the water sensitivity of these

Received: October 11, 2021
Accepted: December 15, 2021
Published: January 14, 2022

materials remained one of the main challenges which hindered their use in different applications, especially packaging since the films lose significant strength after exposure to water and humid environments. Another obstacle in creating robust polysaccharide-based films is the challenge of creating films that display both stiffness and elasticity at the same time. Typically, when plasticizers are added to increase elasticity, some stiffness is also lost. Therefore, we decided to take a different approach. We used metal coordination bonding, relying on the relatively strong supramolecular interactions to make tough water-stable bio-based materials that display mechanical properties comparable to synthetic plastics (Figure 1). Such metal-coordination interactions have been shown to

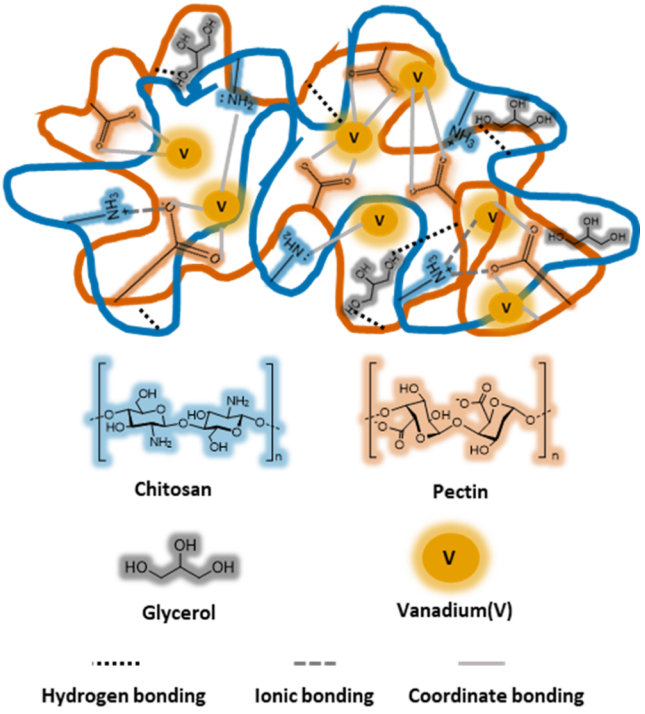

Figure 1. Chemical structures of different components present in the films: CH, PE, glycerol, and sodium metavanadate, and a representation of different supramolecular interactions involved in the formation of the film.

impart new strength and stability to soft materials, including a new photoresponse.[28−35] CH and PE were chosen because they are known to form films when mixed through their oppositely charged groups $-NH_3^+$ and $-COO^-$, respectively.[36] CH is a linear polysaccharide obtained from chitin by deacetylation and processed from the shell of crustaceans and is the second most abundant naturally occurring polysaccharide.[37] PE is a heterogeneously branched polysaccharide mainly composed of galacturonic acid units and is found in the cell wall of most plants.[38] For the metal coordination interactions, we chose vanadium metal ions because we were inspired by catechol−metal coordination interactions present in marine biological systems such as mussels and ascidians.[39,40] In addition, the vanadium ion in its +5-oxidation state is stable and water soluble[41] and showed photoreactivity with some ligands.[42] Previously in our lab, we made and studied vanadium(V)-tartrate complexes.[43] We showed that these complexes undergo a photochemical reaction which reduces V(V) to V(IV). We wanted to combine the advantages offered by metal coordination for more robust materials with the photochemistry of vanadium complexes to create polysaccharide-based films with unique mechanical and photochemical properties. In this paper, we report that V(V) coordination in CH/PE polysaccharide films allows for mechanically strong materials, even in water, that also show photochemistry with striking changes in color observed during light irradiation.

MATERIALS AND METHODS

Materials. CH [deacetylated chitin, poly(D-glucosamine)] with a low molecular weight of 50,000−190,000 Da (lot# 448869), PE from citrus peel with >74% galacturonic acid (lot# P9135), and sodium metavanadate (≥98% purity) were purchased from Sigma-Aldrich. Concentrated hydrochloric acid (HCl) was obtained from EMD Millipore Corporation. Sodium hydroxide pellets low in carbonate was purchased from Millipore Sigma. Glycerol certified ACS was purchased from Fischer Chemical. Potassium bromide crystals were purchased from Baker & Adamson Reagents, General Chemical Division. All chemicals were used as received. Aqueous solutions were prepared using deionized water.

Preparation of PE/CH/Glycerol Composite Films. Equal amounts of PE and CH were dissolved in 0.1 M HCl solution to yield a total polymer concentration of 1.5% by weight, typically 0.3 g of PE and 0.3 g of CH are mixed in 40 mL of 0.1 M HCl. PE was added first to the Erlenmeyer flask containing the HCl solution. The Erlenmeyer flask was placed in a water bath at 80 °C, and the solution was stirred for 30 min using a magnetic stirrer. CH was added next, and the solution was stirred for an additional 2.5 h. Finally, glycerol (mass ratio of PE/CH/glycerol 1:1:4 on a dry basis of the weight of PE and CH) was added (typically 1.2 g or 0.95 mL) to the flask, and the solution was stirred for another 15 min. The resulting homogeneous solution was sonicated in an ultrasonic bath to remove air bubbles. 10 mL of the solution was poured in a Teflon mold (70 mm × 70 mm × 1.95 mm) and air dried for 3−4 days at room temperature. The obtained film was denoted as the control film.

Incorporation of V(V) into PE/CH/Glycerol Composite Films. Sodium metavanadate was used as a source for the V(V) metal ion. 20 mM of sodium metavanadate solution was prepared by dissolving an appropriate amount of the powder in deionized water at 60 °C. 25 mL of the V(V) solution was poured in a large Petri dish. The control film was soaked in the solution for 5 min and then air-dried. The resulting V(V)-containing film was denoted as the V(V) film.

Fourier Transform Infrared Spectroscopy. KBr pellets were prepared by mixing 10 mg of the compound to be analyzed (CH and PE) with 65 mg of KBr powder in a mortar. As for the films, they were cut into tiny pieces and mixed with KBr. The mixture was ground into a fine powder using a pestle. Then, the pellets were made using a dry pellet pressing die set. For irradiation experiments, the V(V) film was clamped and subjected to irradiation using 405 nm light (145 mW/cm^2) for increasing periods of time. The clamp was then placed in the instrument to collect the spectra. Spectra were collected using a Shimadzu FTIR-8400 S instrument combined with IRsolution software.

Scanning Electron Microscopy and Elemental Mapping. The films were cut into small pieces for cross-section examination. Samples were sputter-coated with Au/Pd using a Polaron sputter coater for 2.5 min. SEM images were obtained using a Hitachi S-2700 scanning electron microscope at 12 kV for V films and 6 kV for control films.

Mapping of V element was also performed using energy-dispersive X-ray spectroscopy. An energy-dispersive X-ray analysis detecting unit (model: PV77-47700-ME) was used. The images were collected at a resolution of 256 × 200 pixels.

Images and mapping were obtained for control films, dark samples [non-irradiated V(V) films], and for V films irradiated with a 405 nm light emitting diode (LED) source (145 mW/cm^2).

Lamellar distances were determined from the SEM images by ImageJ. Multiple straight lines were drawn between two sheets and

https://doi.org/10.1021/acsapm.1c01371
ACS Appl. Polym. Mater. 2022, 4, 859−867

then the length of each line was determined using the scale present on the SEM image. Histograms of lamellar distance were determined from 0 with a bin size of 0.05 μm, and number of bins was chosen to be 50.

Mechanical Property Characterization of Films. Mechanical properties were measured using a TA Instruments Discovery HR-2 rheometer operating in the DMA mode. Two attachments, a tension fixture and a dual cantilever, were used to conduct the measurements.

Dual Cantilever Measurements. The V(V) films were cut into small rectangular strips (~60.00 mm × 15.00 mm). A frequency sweep test was performed where the sample was suggested to an axial tension force of 0.5 N. The frequency was increased from 0.05 to 0.5 Hz. The axial displacement was fixed at 100 μm. Storage (G') and loss (G'') moduli were obtained over this range. This test was performed on dry V(V) films and on V(V) films soaked in water for different times.

Tension Fixture Measurements. The control and V(V) films were cut into small rectangular strips (~30.00 mm × 6.50 mm). A time sweep test was performed where a tension stress of 0.5 N was applied on the samples with a constant frequency of 1 Hz and an axial displacement of 50 μm. Storage (G') and loss (G'') moduli were obtained over time. Another experiment was performed where the V(V) film was subjected to continuous irradiation with a 405 nm LED source (145 mW/cm^2), and a time sweep test was done with the same conditions stated above but no force was applied.

All the measurements were performed at room temperature (20 °C).

Thermogravimetric Characterization of Films. Control and V(V) films were cut into very small pieces using scissors. A few milligrams (~2−12 mg) were placed in alumina crucibles and subjected to a temperature range of 25−1000 °C at a heating rate of 10 °C/min. A HITACHI STA7200 thermal analysis system was used to obtain the measurements.

Diffuse Reflectance Spectroscopy. The V(V) films were cut into small rectangular strips (~30.00 mm × 12.50 mm). One strip was irradiated with a 405 nm LED source (145 mW/cm^2). Changes in color accompanying irradiation were monitored using diffuse reflectance spectroscopy. In brief, a white light generated by a halogen light source (HL-2000-FHSA, Ocean Optics) was sent to illuminate the sample through an optic fiber. The reflected light was delivered back to a miniature spectrometer from Ocean Optics Flame. A diffuse reflectance spectrum, which represents the changes in % reflection versus wavelength, was obtained.

RESULTS AND DISCUSSION

We were successfully able to prepare composite films using PE, CH, and glycerol that were relatively robust and elastic. Most of the polysaccharide-based films are too brittle for two main reasons. First, the presence of extensive intermolecular interactions which hold the polymeric chains together decreases the elasticity of the material. Second, a decrease in humidity levels causes stiffening of the films due to the evaporation of water molecules trapped inside the polymeric network which act as a plasticizer.[44] Therefore, glycerol was added to act as a plasticizer to reduce the brittleness of the material. An acidic solution was used as the solvent to protonate the amine groups of CH and make it water soluble. Under neutral or basic conditions, CH has free amino groups which reduce its solubility in water.[45] The film formation was due to hydrogen bonding between the two polymers and glycerol as well as ionic interactions between the $-NH_3^+$ and $-COO^-$ moieties present in CH and PE, respectively.

To enhance the water stability and mechanical properties of the CH/PE control films, they were soaked in sodium metavanadate solution which contains the V(V) metal ion. The control film which was initially colorless turned yellow after soaking it in V(V) solution, indicating the successful incorporation of the metal into the film and likely complexation by the carboxylate and amine groups of the PE and CH, respectively (Figures 1 and 2). By touch, the dried film

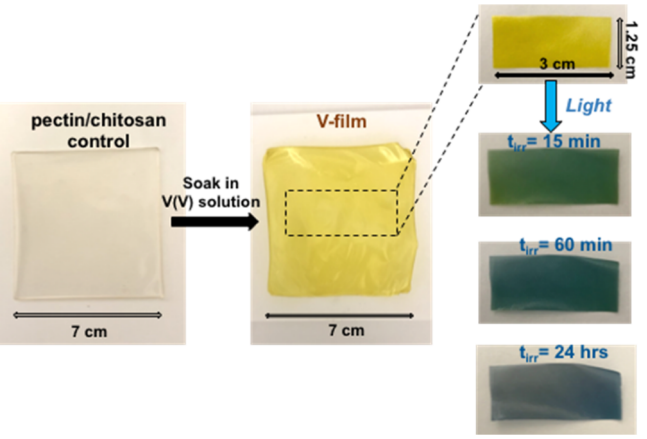

Figure 2. Change in the color of the control film upon incorporation of the vanadium ion and upon irradiation of the V(V) film with a 405 nm LED source (145 mW/cm^2) for increasing periods of time.

containing the vanadium was stiffer than the control film and less stretchy, which could be explained by the strong intermolecular interactions between the metal ions, the polymers, and glycerol present in the film. The concentration of the vanadium ion and the soaking time were chosen in a way to obtain a film sufficient for mechanical testing. The concentration of the metavanadate ion was chosen to be 20 mM according to the results of preliminary experiments, which showed that with lower concentrations of the V(V) ion, CH precipitated out before the metal bound to it due to the rise in pH, whereas at higher concentrations, the film turned to be very stiff due to extensive metal ion−polymer coordination. As for the soaking time, it was chosen to be 5 min because with longer times more metals would bind to the polymers which will also give stiff films not appropriate for mechanical testing (Table S1). Finally, the ideal glycerol amount added needs to be less than four times the amount of each polymer because otherwise a soggy and overplasticized film was obtained.

In previous work done in our lab, it was shown that V(V) with small molecules hydroxy acids (tartrate) undergoes a photochemical reaction reducing it to V(IV) through an intermediate mixed valent state.[43] We wanted to examine the possibility of having a similar photoreaction of V(V) when coordinated with polysaccharides in the solid state. For that purpose, the V(V)-coordinated film was subjected to irradiation using a 405 nm LED source (145 mW/cm^2). A change in color from yellow to blue was observed, indicating that the photoreduction was taking place inside the film (Figures 2 and S6).

To study the different interactions within the films, the spectra of pure PE, pure CH, the control film, and V(V) coordinated film were obtained (Figure 3A). For pure PE, O−H stretching and C−H stretching of CH_2 group vibrations appeared at 3425 and 2939 cm^{-1}, respectively. The band at 1751 cm^{-1} was attributed to the C═O of the carboxylic groups, while the one at 1620 cm^{-1} resulted from the single C−O$^-$ bond of the carboxylate anions. The shoulders at 1149 and 1103 cm^{-1} were the characteristics of C−O−C stretching vibrations. As for the pure CH, the peak at 3387 cm^{-1} was

https://doi.org/10.1021/acsapm.1c01371
ACS Appl. Polym. Mater. 2022, 4, 859−867

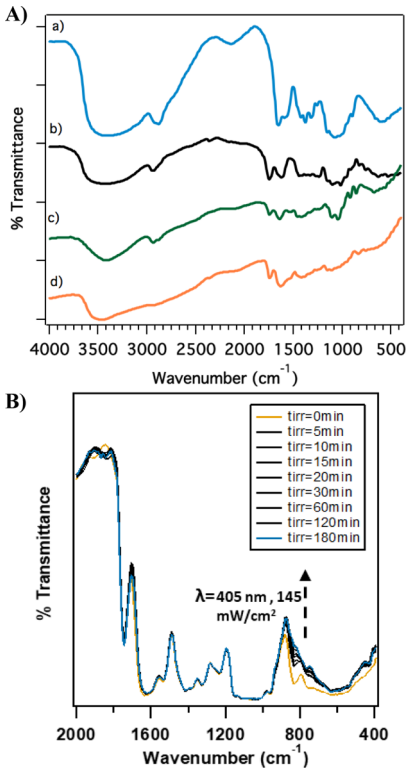

Figure 3. (A) IR spectra of (a) pure CH (blue), (b) pure PE (black), (c) control film (green), and (d) V(V) film (orange). (B) IR spectrum of the V(V) film under irradiation using a 405 nm LED source (145 mW/cm^2) for increasing periods of time.

assigned to O−H stretching, and the one at 2916 cm^{-1} was assigned to symmetric C−H stretching. The peak at 1651 cm^{-1} indicated the vibrations of the carbonyl group, while the one at 1589 cm^{-1} corresponded to N−H bending vibration. These values matched the numbers from previous literature.[46]

When comparing the Fourier transform infrared (FT-IR) spectra of the films to those of pure PE and pure CH, clear shifts were observed. In films, the PE specific peak at 1751 cm^{-1} was shifted to 1743 cm^{-1} for both the control film and V(V) film. The specific peak of CH at 1589 cm^{-1} shifted to 1535 cm^{-1} as well. These shifts were possibly the outcome of the interactions between the two polysaccharides via their oppositely charged groups $-NH_3^+$ and $-COO^-$. Also shifts in the O−H stretching region were observed, indicating the involvement of hydrogen bonding in the interactions. The two peaks at 1111 and 1041 cm^{-1} present in the control film disappeared in the film with V(V), which could be due to the binding of V(V) to the ether oxygen of the ring. The peak at 833 cm^{-1} could be attributed to V−OH vibrations or C−O−C glycosidic linkage.[36,47] Upon irradiation with a 405 nm LED source, the intensity of this peak decreased with increasing irradiation times indicating changes in the interactions inside the film attributed with the photoreduction of V(V) to V(IV) and breaking of the glycosidic bond (Figure 3B). To further prove the presence of interactions between the V(V) ion and the polymers, a solution containing the three components, PE, CH, and glycerol, was prepared, and its viscosity was measured. The metal was then added, and the viscosity of the solution was measured again. An increase in viscosity was observed upon addition of the metal, indicating that the metal is coordinating to the polymers forming a denser and stronger network (Figure S1).

The microstructure within the films was studied using scanning electron microscopy (SEM). The cross-sectional images showed laminated sheets for control and V(V) films (Figure 4A). The presence of both glycerol and vanadium in

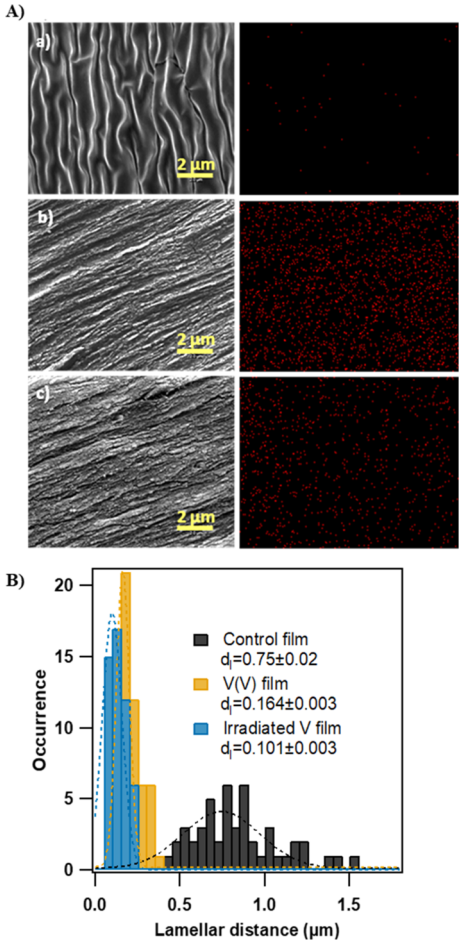

Figure 4. (A) Left: electron micrographs showing the cross section of the (a) control film, (b) V(V) film before irradiation, and (c) V(V) film irradiated for 20 h using a 405 nm LED source (145 mW/cm^2). Right: mapping of the V element inside the same films. (B) Lamellar distance (μm) in control films, dark, and irradiated V(V) films calculated from the SEM images.

the films affected the lamellar distances (Figure 4B). The distance between the sheet-like structures was significantly larger in the control films (~0.75 μm) compared to those with V(V) (~0.16 μm), signaling stronger crosslinking of the polymers through metal coordination. Glycerol as a plasticizer positions itself between the polysaccharide chains and reduces polymer to polymer interactions, increasing the free volume between the polymers. On the other hand, although glycerol is also present in the V(V) film, metal−polymer interactions overcome the effect of glycerol and hold the polymer chains together by reducing the polymer-to-polymer intermolecular distance. Also, we believe that the amount of glycerol was reduced after soaking the control films in vanadium solution due to the high solubility of glycerol in water. The V(V) film was irradiated for increasing periods of time (2 min, 2 h, and 20 h), and SEM images were also collected to study the effect of irradiation on the structure of the material. No remarkable

https://doi.org/10.1021/acsapm.1c01371
ACS Appl. Polym. Mater. 2022, 4, 859−867

changes in morphology, just a small change in the lamellar distance was observed upon irradiation (~0.10 μm for irradiated V(V) film compared to ~0.16 μm for the non-irradiated sample, Figures 4A,B and S2). Vanadium mapping was done to observe the spatial distribution of this metal inside the films. Vanadium was evenly distributed within the non-irradiated film. No change in the metal distribution was observed after irradiation with blue light. Based on the SEM and mapping results, we concluded that irradiation might induce molecular rearrangements within the film but not pronounced enough to cause dramatic changes in the structure of the film or its degradation.

The effect of the addition of V(V) to the film on its mechanical properties was studied using dynamic mechanical analysis (DMA). The storage modulus of the control PE/CH film was much smaller compared to that of the V(V) film, which is in agreement with the IR and viscosity data (Figure 5). V(V) bound to the two polymers increased the stiffness of

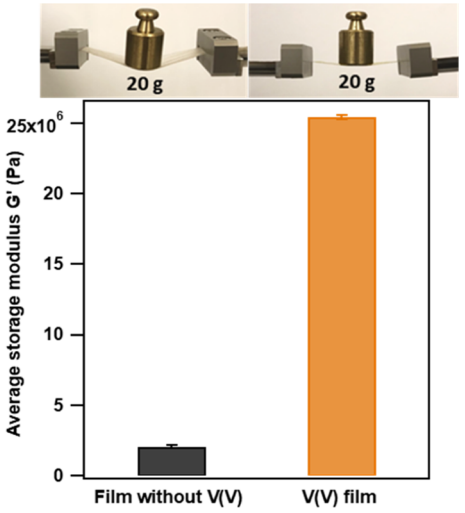

Figure 5. Storage modulus of the control film of CH and PE only (black, left) and the film with V(V) dynamic covalent bonds (orange, right) and their ability to hold weight.

the control film. The difference in stiffness was also visualized by placing a 20 g weight on top of the films. The control films curved downward, whereas the V(V) film remained intact and was able to hold the weight with no changes in its shape (Figure 5).

The stability of the films in water was also studied. The dry V(V) films have a storage modulus around 47.0 MPa. This value of the storage modulus was different from the value that appeared in Figure 5 because a different size sample was used to perform this experiment since a different attachment in the rheometer was used. After soaking the films in deionized water, a significant decrease in storage modulus was observed (Figure 6). Changes in mechanical properties endured by the films were attributed to swelling, from water absorbed by the film until equilibrium was reached. The swelling % of the films was measured with time. An increase in swelling % was observed with increasing soaking time in water (Figure S3). The free hydroxyl and amine groups not involved in the intermolecular interactions between PE and CH can interact with water molecules which causes swelling of the film. In addition, glycerol as a plasticizer is known to increase the intramolecular

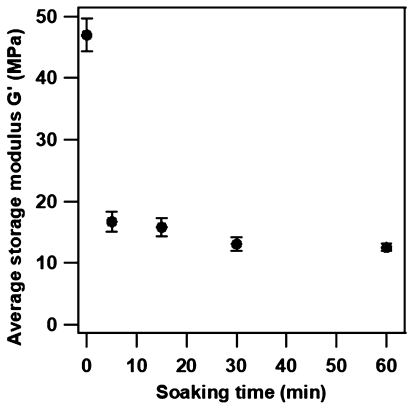

Figure 6. Storage modulus of the film with V(V) coordination with increasing soaking times in water.

distance weakening the polymeric network and facilitating the penetration of water.[48]

Although the storage modulus of the films has decreased, the V(V) films remained in good shape, with a storage modulus still much higher than the control films, and no degradation or significant solubilization was observed. Solubility as determined by weight loss was calculated to be 22.0 ± 1.7, which can be considered low (Table S2). The loss of mass can be attributed to the loss of weakly bound polymers, glycerol, or vanadium ions present on the surface of the film. In addition, as water penetrates the polymer network, it loosens it, leading to the release of the components into water. After the drying process following soaking in water, the films became stiffer. This could be explained by the loss of unbound glycerol, which is the component responsible for enhancing the film flexibility and elasticity. To further study the effect of water on the films, different weights were placed on top of film strips and the amount of bending was measured (Figure S4). Dry films were able to hold more weight than wet films. Compared to the V(V) film, the control film swelled to a huge degree and started disintegrating in water (see the video in the Supporting Information).

Thermal analysis of films was carried out to determine their thermal degradation pattern and the effect of the addition of vanadium metals on thermal stability of the films. It is worthy to underline that CH was more thermally stable than PE (Figure S5); therefore, a film containing both polymers should be more thermally stable than PE or CH alone.[49] However, when comparing thermal gravimetric analysis (TGA) curves of the control film to TGA curves of either PE or CH, the control film showed higher susceptibility to degradation and this was due to the incorporation of glycerol in the film, which reduced the compactness of the film and hence its thermal stability.

To study the effect of vanadium on the thermal stability of the film, we compared TGA and DTA curves of both films (Figure 7). The initial mass loss below 200 °C is endothermic and corresponds to the loss of water and other volatile components for both films. For the control film, the second step degradation reached a maximum at 210 °C. This step which corresponds to the largest weight loss represents PE depolymerization. The third step degradation at 295 °C corresponds to amine decomposition, and it is a very small weight loss. The fourth step degradation at 448 °C might be due to the decomposition of $-CH_2OH$ groups. The total degradation of the ring structure is responsible for the appearance of the fifth degradation step at 554 °C.[19,50,51] As

https://doi.org/10.1021/acsapm.1c01371
ACS Appl. Polym. Mater. 2022, 4, 859−867

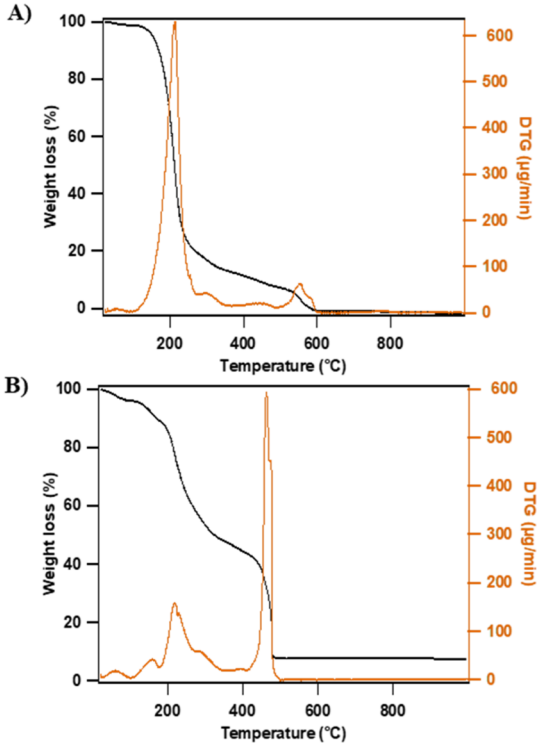

Figure 7. TGA and DTG patterns for the (A) control film of CH and PE only and the (B) film with V(V) dynamic covalent bonds.

for the V(V) film, the second and third degradation steps at 218 and 462 °C, respectively, appear at higher temperatures than the control film. The largest weight loss for the V(V) film was observed in the third step and was strongly exothermic. This degradation step also involved the breaking of coordinate V-polymer bonds. Increase in thermal stability is caused by the compact structure of the (V) film created by the increase in intermolecular interactions upon the addition of the metal. Unlike the metal-free films where all mass was burned off during the experiment, the V(V) film showed a final mass of approximately 10%, indicating residual vanadium remaining, likely as vanadium oxide species.

To determine the effect of light on the mechanical properties of the V(V) film, the latter was mounted on the grips of the tension fixture and irradiated while performing a time sweep test. Before irradiation and for the first 5 min, no significant change in storage modulus was observed. Once the light was turned on, an abrupt decrease in storage modulus was observed followed by a fast increase and then formation of a plateau at higher modulus. This might be due to some rearrangements taking place inside the film, maybe breaking of polymer bonds accompanying the reduction of V(V) to V(IV) and formation of new bonds with V(IV). We attribute these changes primarily to the rearrangement after the photoreaction and not just stronger coordination to V(IV) because in aqueous solutions, irradiation of the CH/PE solutions with V(V) leads to a simple decrease in viscosity (Figure S1). To prove that those changes were due to the presence of vanadium inside the film, the same experiment was run with the control film. No immediate change in storage modulus was observed after irradiation but a small decrease was observed with time due to exhaustion of the film (Figure 8).

It is worth mentioning that the initial storage modulus is different for the three V(V) film samples, and this is because

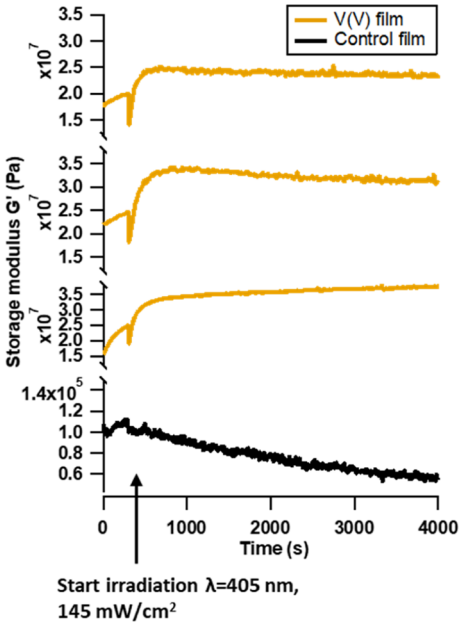

Figure 8. Monitoring changes in storage modulus in real time of the control film (bottom, black) and three different V(V) films (top, gold) upon irradiation with a 405 nm LED source (145 mW/cm^2).

no force was applied on the films when running the measurements. With long measurements and under an applied force, the films tend to break after being exhausted.

To characterize the photochemistry inside the films, the V(V) films were subjected to irradiation and color changes were monitored using diffuse reflectance spectroscopy. The film which was initially yellow turned green and then blue, which indicated the occurrence of the photochemical reaction which reduced V(V) to V(IV) which is blue in color (Figure S6). An increase in % reflection was observed with irradiation around the 700 nm region accompanied by a decrease of the peak around 450 nm and a small blue shift (Figure 9). Also,

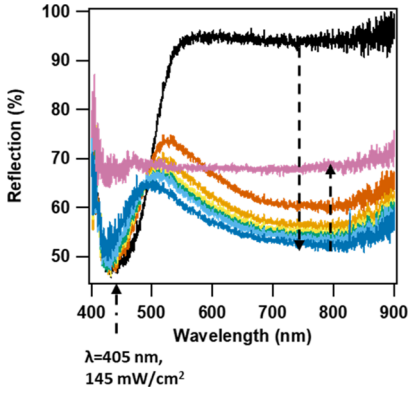

Figure 9. Changes in color of the V(V) film upon irradiation with a 405 nm LED source (145 mW/cm^2) monitored using diffuse reflectance spectroscopy.

averages of R, G, B color analysis values were determined using ImageJ. R and G values were decreasing with irradiation while B values were increasing except for the last sample irradiated for 24 h which was accompanied by a small increase in the R value. The two blue colors observed at 60 min and 24 h are not the same (Figure S7). It should be noted that the high

https://doi.org/10.1021/acsapm.1c01371
ACS Appl. Polym. Mater. 2022, 4, 859−867

intensity LED light is able to fully penetrate through the thin film (Figure S8), and a pattern can be created on the film using a photomask, where the front and back of the film both showed the characteristic dark blue photoproduct in the areas that were irradiated (Figure S9).

CONCLUSIONS

In summary, we were able to show that metal coordination bonding of the vanadium ion can be used to enhance the mechanical and photochemical properties of polysaccharide-based materials as well as their water and thermal stability. This was done by creating films using two natural polysaccharides PE and CH and adding glycerol to act as a plasticizer. To give these materials their unique properties, the V(V) metal ion was incorporated using the soaking method. FT-IR was used to prove the formation of both hydrogen bonding and ionic interactions between the polymers and glycerol and to show the presence of coordinate covalent bonding between V(V) and the polymers. These interactions lead to enhanced mechanical properties of V(V) films compared to control films. This was reflected by the increase in stiffness and water stability. Also, the stiffness decreases with increasing soaking time in water due to swelling. Interestingly, these films showed photochemistry upon light irradiation due the presence of V(V), which was reduced to V(IV). SEM images showed no significant differences in structure with irradiation but only a small change in the lamellar distance. Diffuse reflectance measurements showed that films turned green and then blue with irradiation, corresponding to the photochemical reduction of V(V) to V(IV), which is blue in color. Metal coordination is a powerful tool to create robust bioplastics and to impart photoreactivity in materials. We used V(V) photochemistry to pattern films and create regions of different colors. These films might be also used for different types of packaging except for food packaging since V(V) is known to be toxic at high concentrations.[52]

ASSOCIATED CONTENT

Supporting Information

The Supporting Information is available free of charge at https://pubs.acs.org/doi/10.1021/acsapm.1c01371.

Water stability and stiffness of a V(V) film compared to the control film (MOV)

Experimental conditions for making films, viscosity measurements, SEM analysis, swelling and solubility % calculations, TGA, and pictures of films and color analysis of films and light irradiation (PDF)

AUTHOR INFORMATION

Corresponding Author

Alexis D. Ostrowski − *Department of Chemistry and Center for Photochemical Sciences, Bowling Green State University, Bowling Green, Ohio 43403, United States;* orcid.org/0000-0002-3207-1845; Email: alexiso@bgsu.edu

Authors

Carina Haddad − *Department of Chemistry and Center for Photochemical Sciences, Bowling Green State University, Bowling Green, Ohio 43403, United States*

E. A. Kalani D. Edirisinghe − *Department of Chemistry and Center for Photochemical Sciences, Bowling Green State University, Bowling Green, Ohio 43403, United States*

Hope M. Brown − *Department of Chemistry and Center for Photochemical Sciences, Bowling Green State University, Bowling Green, Ohio 43403, United States*

Complete contact information is available at: https://pubs.acs.org/10.1021/acsapm.1c01371

Author Contributions

The manuscript was written through contributions of all authors.

Funding

This work was supported by an NSF CAREER award to ADO, Division of Chemistry, Chemical Structure, Dynamics and Mechanisms-B Program and Division of Materials Research Polymers program (CHE-1653892). Additional support was provided to CH by the Herman Frasch Foundation for Chemical Research (811-17F) and to HMB by the BGSU Department of Chemistry summer research fellowship and the BGSU CURS program. ADO also thanks the Dr. Thomas J. Kinstle Professorship at BGSU for support of this project.

Notes

The authors declare no competing financial interest.

ACKNOWLEDGMENTS

We thank Dr. Marilyn Cayer for her help with electron scanning microscopy. We thank Dr. Joseph C. Furgal and the graduate student Nai-hsuan Hu for their help with TGA. We also thank Charles Codding for making the Teflon molds and the diffuse reflectance setup.

ABBREVIATIONS

PE, pectin; CH, chitosan; HCl, hydrochloric acid; KBr, potassium bromide; FT-IR, Fourier transform infrared spectroscopy; SEM, scanning electron microscopy; EDAX, energy-dispersive X-ray spectroscopy; LED, light emitting diode; DMA, dynamic mechanical analysis; TGA, thermal gravimetric analysis; DTG, differential thermogravimetry; DTA, differential thermal analysis

REFERENCES

(1) Millican, J. M.; Agarwal, S. Plastic Pollution: A Material Problem? *Macromolecules* **2021**, *54*, 4455.

(2) Groh, K. J.; Backhaus, T.; Carney-Almroth, B.; Geueke, B.; Inostroza, P. A.; Lennquist, A.; Leslie, H. A.; Maffini, M.; Slunge, D.; Trasande, L.; Warhurst, A. M.; Muncke, J. Overview of Known Plastic Packaging-Associated Chemicals and Their Hazards. *Sci. Total Environ.* **2019**, *651*, 3253−3268.

(3) Kim, S.-J.; Ustunol, Z. Solubility and Moisture Sorption Isotherms of Whey-Protein-Based Edible Films as Influenced by Lipid and Plasticizer Incorporation. *J. Agric. Food Chem.* **2001**, *49*, 4388−4391.

(4) Bravin, B.; Peressini, D.; Sensidoni, A. Influence of Emulsifier Type and Content on Functional Properties of Polysaccharide Lipid-Based Edible Films. *J. Agric. Food Chem.* **2004**, *52*, 6448−6455.

(5) Ferreira, A. R. V.; Alves, V. D.; Coelhoso, I. M. Polysaccharide-Based Membranes in Food Packaging Applications. *Membranes* **2016**, *6*, 22.

(6) Picchio, M. L.; Linck, Y. G.; Monti, G. A.; Gugliotta, L. M.; Minari, R. J.; Alvarez Igarzabal, C. I. Casein Films Crosslinked by Tannic Acid for Food Packaging Applications. *Food Hydrocolloids* **2018**, *84*, 424−434.

(7) González, A.; Gastelú, G.; Barrera, G. N.; Ribotta, P. D.; Álvarez Igarzabal, C. I. Preparation and Characterization of Soy Protein Films Reinforced with Cellulose Nanofibers Obtained from Soybean By-Products. *Food Hydrocolloids* **2019**, *89*, 758−764.

(8) Nešić, A.; Cabrera-Barjas, G.; Dimitrijević-Branković, S.; Davidović, S.; Radovanović, N.; Delattre, C. Prospect of Polysaccharide-Based Materials as Advanced Food Packaging. *Molecules* **2019**, *25*, 135.
(9) Hu, Z.; Hong, P.; Liao, M.; Kong, S.; Huang, N.; Ou, C.; Li, S. Preparation and Characterization of Chitosan—Agarose Composite Films. *Materials* **2016**, *9*, 816.
(10) Ren, L.; Yan, X.; Zhou, J.; Tong, J.; Su, X. Influence of Chitosan Concentration on Mechanical and Barrier Properties of Corn Starch/Chitosan Films. *Int. J. Biol. Macromol.* **2017**, *105*, 1636−1643.
(11) Phoeung, T.; Spanedda, M. V.; Roger, E.; Heurtault, B.; Fournel, S.; Reisch, A.; Mutschler, A.; Perrin-Schmitt, F.; Hemmerlé, J.; Collin, D.; Rawiso, M.; Boulmedais, F.; Schaaf, P.; Lavalle, P.; Frisch, B. Alginate/Chitosan Compact Polyelectrolyte Complexes: A Cell and Bacterial Repellent Material. *Chem. Mater.* **2017**, *29*, 10418−10425.
(12) Munhoz, D. R.; Moreira, F. K. V.; Bresolin, J. D.; Bernardo, M. P.; De Sousa, C. P.; Mattoso, L. H. C. Sustainable Production and In Vitro Biodegradability of Edible Films from Yellow Passion Fruit Coproducts via Continuous Casting. *ACS Sustain. Chem. Eng.* **2018**, *6*, 9883−9892.
(13) Sucheta; Rai, S. K.; Chaturvedi, K.; Yadav, S. K. Evaluation of Structural Integrity and Functionality of Commercial Pectin Based Edible Films Incorporated with Corn Flour, Beetroot, Orange Peel, Muesli and Rice Flour. *Food Hydrocolloids* **2019**, *91*, 127−135.
(14) Shin, M.; Lee, H. Gallol-Rich Hyaluronic Acid Hydrogels: Shear-Thinning, Protein Accumulation against Concentration Gradients, and Degradation-Resistant Properties. *Chem. Mater.* **2017**, *29*, 8211−8220.
(15) Wu, H.; Lei, Y.; Lu, J.; Zhu, R.; Xiao, D.; Jiao, C.; Xia, R.; Zhang, Z.; Shen, G.; Liu, Y.; Li, S.; Li, M. Effect of Citric Acid Induced Crosslinking on the Structure and Properties of Potato Starch/Chitosan Composite Films. *Food Hydrocolloids* **2019**, *97*, 105208.
(16) Wilpiszewska, K.; Antosik, A. K.; Zdanowicz, M. The Effect of Citric Acid on Physicochemical Properties of Hydrophilic Carboxymethyl Starch-Based Films. *J. Polym. Environ.* **2019**, *27*, 1379−1387.
(17) Azeredo, H. M. C.; Mattoso, L. H. C.; Wood, D.; Williams, T. G.; Avena-Bustillos, R. J.; McHugh, T. H. Nanocomposite Edible Films from Mango Puree Reinforced with Cellulose Nanofibers. *J. Food Sci.* **2009**, *74*, N31−N35.
(18) Lorevice, M. V.; Otoni, C. G.; Moura, M. R. d.; Mattoso, L. H. C. Chitosan Nanoparticles on the Improvement of Thermal, Barrier, and Mechanical Properties of High- and Low-Methyl Pectin Films. *Food Hydrocolloids* **2016**, *52*, 732−740.
(19) Priyadarshi, R.; Sauraj; Kumar, B.; Negi, Y. S. Chitosan Film Incorporated with Citric Acid and Glycerol as an Active Packaging Material for Extension of Green Chilli Shelf Life. *Carbohydr. Polym.* **2018**, *195*, 329−338.
(20) Liang, T.; Wang, L. Preparation and Characterization of a Novel Edible Film Based on Artemisia Sphaerocephala Krasch. Gum: Effects of Type and Concentration of Plasticizers. *Food Hydrocolloids* **2018**, *77*, 502−508.
(21) Aitboulahsen, M.; Galiou, O. E.; Laglaoui, A.; Bakkali, M.; Zerrouk, M. H. Effect of Plasticizer Type and Essential Oils on Mechanical, Physicochemical, and Antimicrobial Characteristics of Gelatin, Starch, and Pectin-Based Films. *J. Food Process. Preserv.* **2020**, *44*, No. e14480.
(22) Mali, S.; Grossmann, M. V. E. Effects of Yam Starch Films on Storability and Quality of Fresh Strawberries (Fragaria Ananassa). *J. Agric. Food Chem.* **2003**, *51*, 7005−7011.
(23) Sanjurjo, K.; Flores, S.; Gerschenson, L.; Jagus, R. Study of the Performance of Nisin Supported in Edible Films. *Food Res. Int.* **2006**, *39*, 749−754.
(24) Sevilla, M.; Ferrero, G. A.; Fuertes, A. B. One-Pot Synthesis of Biomass-Based Hierarchical Porous Carbons with a Large Porosity Development. *Chem. Mater.* **2017**, *29*, 6900−6907.
(25) Pan, J.; Cao, D.; Ma, X.; Yang, J. Preparation, Characterization and in Vitro Release Properties of Pectin-Based Curcumin Film. *Korean J. Chem. Eng.* **2019**, *36*, 822−827.
(26) Wei, P.; Huang, J.; Lu, Y.; Zhong, Y.; Men, Y.; Zhang, L.; Cai, J. Unique Stress Whitening and High-Toughness Double-Cross-Linked Cellulose Films. *ACS Sustain. Chem. Eng.* **2019**, *7*, 1707−1717.
(27) Höglund, M.; Garemark, J.; Nero, M.; Willhammar, T.; Popov, S.; Berglund, L. A. Facile Processing of Transparent Wood Nanocomposites with Structural Color from Plasmonic Nanoparticles. *Chem. Mater.* **2021**, *33*, 3736−3745.
(28) Harris, R. D.; Auletta, J. T.; Motlagh, S. A. M.; Lawless, M. J.; Perri, N. M.; Saxena, S.; Weiland, L. M.; Waldeck, D. H.; Clark, W. W.; Meyer, T. Y. Chemical and Electrochemical Manipulation of Mechanical Properties in Stimuli-Responsive Copper-Cross-Linked Hydrogels. *ACS Macro Lett.* **2013**, *2*, 1095−1099.
(29) Giammanco, G. E.; Ostrowski, A. D. Photopatterning the Mechanical Properties of Polysaccharide-Containing Gels Using Fe3+ Coordination. *Chem. Mater.* **2015**, *27*, 4922−4925.
(30) Zheng, S. Y.; Ding, H.; Qian, J.; Yin, J.; Wu, Z. L.; Song, Y.; Zheng, Q. Metal-Coordination Complexes Mediated Physical Hydrogels with High Toughness, Stick−Slip Tearing Behavior, and Good Processability. *Macromolecules* **2016**, *49*, 9637−9646.
(31) Schauser, N. S.; Sanoja, G. E.; Bartels, J. M.; Jain, S. K.; Hu, J. G.; Han, S.; Walker, L. M.; Helgeson, M. E.; Seshadri, R.; Segalman, R. A. Decoupling Bulk Mechanics and Mono- and Multivalent Ion Transport in Polymers Based on Metal−Ligand Coordination. *Chem. Mater.* **2018**, *30*, 5759−5769.
(32) Kim, S.; Peterson, A. M.; Holten-Andersen, N. Enhanced Water Retention Maintains Energy Dissipation in Dehydrated Metal-Coordinate Polymer Networks: Another Role for Fe-Catechol Cross-Links? *Chem. Mater.* **2018**, *30*, 3648−3655.
(33) Guo, Y.; Gao, Z.; Liu, Y.; Huang, Z.; Chai, C.; Hao, J. Multiple Cross-Linking-Dominated Metal−Ligand Coordinated Hydrogels with Tunable Strength and Thermosensitivity. *ACS Appl. Polym. Mater.* **2019**, *1*, 2370−2378.
(34) Yang, J.; Li, M.; Wang, Y.; Wu, H.; Zhen, T.; Xiong, L.; Sun, Q. Double Cross-Linked Chitosan Composite Films Developed with Oxidized Tannic Acid and Ferric Ions Exhibit High Strength and Excellent Water Resistance. *Biomacromolecules* **2019**, *20*, 801−812.
(35) Schofield, R. M. S.; Bailey, J.; Coon, J. J.; Devaraj, A.; Garrett, R. W.; Goggans, M. S.; Hebner, M. G.; Lee, B. S.; Lee, D.; Lovern, N.; Ober-Singleton, S.; Saephan, N.; Seagal, V. R.; Silver, D. M.; Som, H. E.; Twitchell, J.; Wang, X.; Zima, J. S.; Nesson, M. H. The Homogenous Alternative to Biomineralization: Zn- and Mn-Rich Materials Enable Sharp Organismal "Tools" That Reduce Force Requirements. *Sci. Rep.* **2021**, *11*, 17481.
(36) Younis, H. G. R.; Zhao, G. Physicochemical Properties of the Edible Films from the Blends of High Methoxyl Apple Pectin and Chitosan. *Int. J. Biol. Macromol.* **2019**, *131*, 1057−1066.
(37) Leceta, I.; Guerrero, P.; de la Caba, K. Functional Properties of Chitosan-Based Films. *Carbohydr. Polym.* **2013**, *93*, 339−346.
(38) Hoagland, P. D.; Parris, N. Chitosan/Pectin Laminated Films. *J. Agric. Food Chem.* **1996**, *44*, 1915−1919.
(39) Park, J. P.; Song, I. T.; Lee, J.; Ryu, J. H.; Lee, Y.; Lee, H. Vanadyl−Catecholamine Hydrogels Inspired by Ascidians and Mussels. *Chem. Mater.* **2015**, *27*, 105−111.
(40) Schmitt, C. N. Z.; Winter, A.; Bertinetti, L.; Masic, A.; Strauch, P.; Harrington, M. J. Mechanical Homeostasis of a DOPA-Enriched Biological Coating from Mussels in Response to Metal Variation. *J. R. Soc. Interface* **2015**, *12*, 20150466.
(41) Kaliva, M.; Giannadaki, T.; Salifoglou, A.; Raptopoulou, C. P.; Terzis, A. A New Dinuclear Vanadium(V)−Citrate Complex from Aqueous Solutions. Synthetic, Structural, Spectroscopic, and PH-Dependent Studies in Relevance to Aqueous Vanadium(V)−Citrate Speciation. *Inorg. Chem.* **2002**, *41*, 3850−3858.
(42) Gáliková, J.; Schwendt, P.; Tatiersky, J.; Tracey, A. S.; Zák, Z. Stereospecific Formation of Dinuclear Vanadium(V) Tartrato Complexes. *Inorg. Chem.* **2009**, *48*, 8423−8430.

https://doi.org/10.1021/acsapm.1c01371
ACS Appl. Polym. Mater. 2022, 4, 859−867

(43) Edirisinghe, E. A. K. D.; Ayodele, M. J.; Saeedi, S.; Brugh, A. M.; Forbes, M. D. E.; White, T. A.; Ostrowski, A. D. Reversible Photochemistry in Vanadium(V) Tartrate Clusters Containing a Mixed−Valent Intermediate. *Inorganic Chemistry*, **2022**, *in press.*
(44) Otoni, C. G.; Avena-Bustillos, R. J.; Azeredo, H. M. C.; Lorevice, M. V.; Moura, M. R.; Mattoso, L. H. C.; McHugh, T. H. Recent Advances on Edible Films Based on Fruits and Vegetables—A Review. *Compr. Rev. Food Sci. Food Saf.* **2017**, *16*, 1151−1169.
(45) Wang, Q. Z.; Chen, X. G.; Liu, N.; Wang, S. X.; Liu, C. S.; Meng, X. H.; Liu, C. G. Protonation Constants of Chitosan with Different Molecular Weight and Degree of Deacetylation. *Carbohydr. Polym.* **2006**, *65*, 194−201.
(46) Chetouani, A.; Follain, N.; Marais, S.; Rihouey, C.; Elkolli, M.; Bounekhel, M.; Benachour, D.; Le Cerf, D. Physicochemical Properties and Biological Activities of Novel Blend Films Using Oxidized Pectin/Chitosan. *Int. J. Biol. Macromol.* **2017**, *97*, 348−356.
(47) Guimond, S.; Abu Haija, M.; Kaya, S.; Lu, J.; Weissenrieder, J.; Shaikhutdinov, S.; Kuhlenbeck, H.; Freund, H.-J.; Döbler, J.; Sauer, J. Vanadium Oxide Surfaces and Supported Vanadium Oxide Nanoparticles. *Top. Catal.* **2006**, *38*, 117−125.
(48) Basiak, E.; Lenart, A.; Debeaufort, F. How Glycerol and Water Contents Affect the Structural and Functional Properties of Starch-Based Edible Films. *Polymers* **2018**, *10*, 412.
(49) Šešlija, S.; Nešić, A.; Škorić, M. L.; Krušić, M. K.; Santagata, G.; Malinconico, M. Pectin/Carboxymethylcellulose Films as a Potential Food Packaging Material. *Macromol. Symp.* **2018**, *378*, 1600163.
(50) Ghaffari, A.; Navaee, K.; Oskoui, M.; Bayati, K.; Rafiee-Tehrani, M. Preparation and Characterization of Free Mixed-Film of Pectin/Chitosan/Eudragit® RS Intended for Sigmoidal Drug Delivery. *Eur. J. Pharm. Biopharm.* **2007**, *67*, 175−186.
(51) Georgieva, V.; Zvezdova, D.; Vlaev, L. Non-Isothermal Kinetics of Thermal Degradation of Chitosan. *Chem. Cent. J.* **2012**, *6*, 81.
(52) Zwolak, I. Protective Effects of Dietary Antioxidants against Vanadium-Induced Toxicity: A Review. *Oxid. Med. Cell. Longev.* **2020**, *2020*, 1490316.

https://doi.org/10.1021/acsapm.1c01371
ACS Appl. Polym. Mater. 2022, 4, 859−867